Randomized or Probabilistic Hough Transform: Unified Performance Evaluation

Nahum Kiryati [1]

Dept. of Electrical Engineering–Systems, Tel Aviv University, Tel Aviv 69978, Israel

Heikki Kälviäinen and Satu Alaoutinen

Dept. of Information Technology, Lappeenranta University of Technology, P.O. Box 20, FIN-53851 Lappeenranta, Finland

Abstract

Rapid computation of the Hough Transform is necessary in very many computer vision applications. One of the major approaches for fast Hough Transform computation is based on the use of a small random sample of the data set rather than the full set. Two different algorithms within this family are the Randomized Hough Transform (RHT) and the Probabilistic Hough Transform (PHT). There have been contradictory views on the relative merits and drawbacks of the RHT and the PHT. In this paper a unified theoretical framework for analyzing the RHT and the PHT is established. The performance of the two algorithms is characterized both theoretically and experimentally. Clear guidelines for selecting the algorithm that is most suitable for a given application are provided. We show that, when considering the basic algorithms, the RHT is better suited for the analysis of high quality low noise edge images, while for the analysis of noisy low quality images the PHT should be selected.

Key words: Performance evaluation, Probabilistic Hough Transform (PHT), Randomized Hough Transform (RHT)

1. Introduction

The meaningful grouping of points in edge images is the key to various high level tasks in computer vision. The well known Hough Transform is the usual approach for detecting parametric curves or other predefined shapes in a planar set of points. The Duda and Hart [1] formulation of the straight line Hough Transform is commonly referred to as the Standard Hough Transform (SHT).

In the SHT, each of the M data points (x_i, y_i) is transformed to a sinusoidal voting pattern

$$\rho = x_i \cos\theta + y_i \sin\theta \tag{1}$$

in an $N_\theta \times N_\rho$ accumulator array that represents the (θ, ρ) normal parameters plane. The sinusoids that correspond to collinear data points ideally intersect at a single point in the parameter space. This leads to a peak in the accumulator array that is found by search.

Many variations of the Hough Transform have been suggested. According to one classification, the SHT is a *one to many* $(1 \rightarrow m)$ algorithm, in the

[1] Corresponding author. Fax: +972 3 640 7095. E-mail: nk@eng.tau.ac.il

sense that one data point votes for many accumulators. In a *many to one* ($m \rightarrow 1$) algorithm for straight line detection, each of the $M(M-1)/2$ *pairs* of data points defines a line and thus votes for a single accumulator. $1 \rightarrow 1$ and $m \rightarrow m$ algorithms also exist but will not be discussed here.

The Hough Transform can be regarded as a systematic way to carry out exhaustive search in a discretized pattern space. As an exhaustive search technique, the Hough Transform is robust but computationally demanding. Driven by the significant practical need, the development of algorithms for fast computation of the Hough Transform and the evaluation of their performance is an active, ongoing process.

The probabilistic/randomized Hough Transform [2,3,6,10,11] is based on the observation that, in many cases, complete accumulation of evidence in the voting stage of the Hough transform is not necessary for the reliable detection of shapes. Significant computational savings are obtained by replacing full voting by a limited poll, i.e., by using just a subset of the data points for voting. The Randomized Hough Transform (RHT) [10,11] is an $m \rightarrow 1$ algorithm in which pairs of points are randomly selected. In [3,4], extensions of the RHT have been proposed using, for example, the windowing of an image randomly and relying on the connectivity of neighboring points. The Probabilistic Hough Transform (PHT) [2] is a $1 \rightarrow m$ algorithm. It is similar to the SHT but uses just a small random subset of the data points. The possibility of online adaptation of the poll size to the complexity of the detection task has been demonstrated in [12] and analyzed in [9] using sequential analysis techniques. Various modifications, extensions and applications of the generic algorithms have been described. In this paper, we consider the basic versions of the RHT and PHT.

There have been contradictory views on the relative merits and drawbacks of the RHT and PHT. The purpose of this paper is to set a unified framework for the analysis of the RHT and PHT and to provide guidelines for using the best algorithm in a given application. The theoretical results are supported by experiments. Preliminary results appeared in [5].

2. PHT Analysis

Consider an edge image with S points on an ideal line and N randomly distributed noise points. Let $M = S + N$ denote the total number of points in the image. In the PHT [2], m points [2] are randomly chosen (with redraw). Of these, let s denote the number of points that belong to the line. The PHT will fail in either of the following situations:

- When $s \leq 2$, since any two points define a line. This means that the peak in the accumulator array that corresponds to the actual line will be buried in the noise. To succeed, it is necessary to have $s \geq 3$.
- When $s \geq 3$, if some of the randomly distributed noise points are, by chance, collinear, and a few of those points were selected to take part in the PHT poll.

In a finite set of points that are randomly distributed in a continuous image support, with probability 1 there are no collinear subsets (of cardinality that is greater than 2). If the image support is discrete, there is some finite probability for the existence of random collinear subsets. But if the total number of points that are selected to be in the PHT poll is small, it can still be assumed that the probability of picking a "random coalition" is negligible. We therefore assume that the PHT will fail only when $s \leq 2$. Thus, the probability of PHT failure is

$$\Pr(s \leq 2) = \sum_{k=0}^{2} \binom{m}{k} \left(\frac{S}{M}\right)^k \left(1 - \frac{S}{M}\right)^{m-k} \quad (2)$$

Suppose now that the line in the image is not ideal, i.e., that the actual positions of the line points deviate from their "true" locations (due to, say, edge detector errors or just due to spatial discretization). Complete analysis of this situation is not easy, see e.g. [8]. A crude model for the effect of location errors is that only αS $(0 < \alpha < 1)$ of

[2] The poll size m is commonly set to some fixed conservative value. However, it is now known that adaptive, data-driven setting of the poll size [9,12] leads to polls that are on average smaller than the fixed poll that leads to the same error rate. The following analysis regards the poll size as a parameter.

the S ideal line points remain sufficiently close to the line, and can still be considered to belong to the line. The rest, according to the model, are considered as an addition to the group of randomly located noise points. Using this model, the probability of PHT failure is

$$\Pr(s \leq 2) = \sum_{k=0}^{2} \binom{m}{k} \left(\frac{\alpha S}{M}\right)^k \left(1 - \frac{\alpha S}{M}\right)^{m-k} \quad (3)$$

The fraction of data points in the image that effectively belong to the line, $\alpha S/M$, quantifies the difficulty of the line detection task. Being interested in performance evaluation, we generally assume that $\alpha S/M \ll 1$, i.e., that the task is a difficult one. The performance of the PHT depends on $m\alpha S/M$, the expected value of s. There are two main cases:

(1) A PHT poll size m that is too small, in the sense that $m\alpha S/M \ll 1$. In this case, the probability of PHT failure is close to 1:

$$\Pr(s \leq 2) \approx \left(1 - \frac{\alpha S}{M}\right)^m \approx 1 - m\frac{\alpha S}{M} \approx 1 \quad (4)$$

(2) A PHT poll size m that is sufficiently large, leading to $m\alpha S/M \gg 1$. This is the normal operating domain of the PHT[3]. Here the probability of PHT failure is

$$\Pr(s \leq 2) \approx \left(1 - \frac{\alpha S}{M}\right)^{m-2} \cdot \frac{m^2}{2} \cdot \left(\frac{\alpha S}{M}\right)^2 \quad (5)$$

By taking the derivative with respect to m, it is easy to show that the probability decreases as a function of m for $m\alpha S/M > 2$.

We proceed to calculate how large the poll size m should be in order to obtain some small probability of failure ϵ. Starting from Eq. 5, using the identity $a^m = e^{m \ln a}$ and the 1st order Taylor approximation $\ln(1 + x) \approx x$ (that holds for small $|x|$), we obtain

$$\epsilon \approx \frac{1}{2} e^{-c} c^2 \quad (6)$$

where $c \equiv m\alpha S/M$. Numerical solutions of Eq. 6 for several values of ϵ are shown in Table 1.

[3] The transition region, where $m\alpha S/M \approx 1$, is not of practical interest.

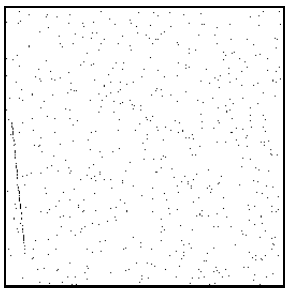

Fig. 1. A 256×256 test image, with $S = 64$ points on a digital line, and $N = 576$ randomly distributed noise points; $S/M = 0.1$.

Consider the 256×256 edge image shown in Fig. 1. It contains a digital straight line from which half of the points have been deleted, leaving $S = 64$ line points, and $N = 576$ randomly distributed noise points. The total number of points is thus $M = S + N = 640$. The top row in Table 2 shows the empirical poll sizes m needed to achieve several PHT failure rates ϵ. The bottom row in Table 2 shows the values of m that are necessary to obtain those failure rates, as predicted from Table 1 using $\alpha = 0.68$.

The "correct" value of α, that best predicts (or explains) the empirical findings, is influenced by various factors, especially by deviations from the assumptions that were made in the analysis. Nevertheless, based on this and other experiments, it is seen that Eqs. 5 and 6 provide valuable insights and useful theoretical predictions of the performance of the PHT.

Table 1
The required value of $m\alpha S/M$ in the PHT as a function of the failure rate ϵ.

ϵ	0.1	0.03	0.01	0.001	0.0001
$c \equiv m\alpha S/M$	4.70	6.58	8.09	11.01	13.76

Table 2
Empirical and theoretical poll sizes, for several failure rates, in the application of the PHT to the edge image shown in Fig. 1.

ϵ	0.1	0.03	0.01
Empirical m	67	106	111
Predicted m	69	97	119

3. RHT Analysis

Consider again an edge image with S points on an ideal line and N noise points that are randomly distributed. Let $M = S+N$ denote the total number of points in the image.

In the RHT, *p pairs* of points [4] are chosen at random (with redraw) to take part in the poll. Among them, let l denote the number of pairs in which both points are on the line. The RHT will fail in one of the following cases:

- When $l \leq 1$, since even with $l = 1$ it will not be possible to distinguish the pair of points that belong to the line from all other pairs. To succeed, it is necessary to have $l \geq 2$.
- When $l \geq 2$, if the line parameters defined by two (or more) of the other (non-line) pairs that take part in the poll accidently coincide.

In a continuous image support, there is zero probability for random collinear alignment of two non-line pairs. In a discrete image, the probability can be considered negligible as long as the RHT poll size is small. We therefore assume that the RHT will fail only when $l \leq 1$. Thus, the probability of RHT failure is

$$\Pr(l \leq 1) = \sum_{k=0}^{1} \binom{p}{k} \left[\left(\frac{S}{M}\right)^2\right]^k \left[1 - \left(\frac{S}{M}\right)^2\right]^{p-k} \quad (7)$$

Suppose again that the line in the image is not ideal, i.e., that the actual positions of the line points deviate from their true locations. We maintain the crude model that only αS $(0 < \alpha < 1)$ of the S ideal line points remain sufficiently close to the line, and the rest can be added to the group of randomly located noise points. Using this model, the probability of RHT failure is

$$\Pr(l \leq 1) = \sum_{k=0}^{1} \binom{p}{k} \left[\left(\frac{\alpha S}{M}\right)^2\right]^k \left[1 - \left(\frac{\alpha S}{M}\right)^2\right]^{p-k} \quad (8)$$

As in the analysis of the PHT, we generally assume that the line detection task is a difficult one, i.e., $\alpha S/M \ll 1$. The performance of the RHT depends on $p(\alpha S/M)^2$, the expected value of l. Here too there are two main cases:

(1) A RHT poll size p that is too small, in the sense that $p(\alpha S/M)^2 \ll 1$. In this case, the probability of RHT failure is close to 1:

$$\Pr(l \leq 1) \approx 1 - p\left(\frac{\alpha S}{M}\right)^2 \approx 1 \quad (9)$$

(2) A RHT poll size p that is sufficiently large, leading to $p(\alpha S/M)^2 \gg 1$. This is the normal operating domain of the RHT. Here the probability of RHT failure is

$$\Pr(l \leq 1) \approx \left[1 - \left(\frac{\alpha S}{M}\right)^2\right]^{p-1} \cdot p \cdot \left(\frac{\alpha S}{M}\right)^2 \quad (10)$$

We proceed to calculate how large the RHT poll size (i.e., the number of pairs p) must be to obtain some small probability of failure ϵ. Beginning with Eq. 10, using the identity $a^p = e^{p \ln a}$ and the 1st order Taylor approximation $\ln(1+x) \approx x$ (that holds for small $|x|$), we obtain

$$\epsilon \approx e^{-b} \cdot b \quad (11)$$

where $b \equiv p(\alpha S/M)^2$. Numerical solutions of Eq. 11 for several values of ϵ are shown in Table 3.

Consider again the 256×256 edge image shown in Fig. 1. The top row in Table 4 shows the empirical RHT poll sizes p (pairs) needed to achieve several RHT failure rates ϵ. The bottom row in Table 4 shows the values of p that are necessary to obtain those failure rates, as predicted from Table 3 using $\alpha = 0.71$.

The value of α that best explains the empirical findings is again influenced by various factors.

Table 3
The required value of $p(\alpha S/M)^2$ in the RHT as a function of the failure rate ϵ.

ϵ	0.1	0.03	0.01	0.001	0.0001
$b \equiv p(\alpha S/M)^2$	3.58	5.14	6.47	9.11	11.67

[4] In the RHT, polling is stopped when the highest peak in the accumulator array reaches a threshold. This is, in fact, an adaptive stopping rule that is known in the statistical literature as the *inverse sampling* rule [9]. In the following analysis, the poll size p is regarded as a parameter.

Table 4
Empirical and theoretical RHT poll sizes (pairs), for several failure rates, in the application of the RHT to the edge image shown in Fig. 1.

ϵ	0.1	0.03	0.01
Empirical p	775	987	1205
Predicted p	710	1019	1283

However, the analysis, as summarized by Eqs. 10 and 11, provides useful insights and theoretical predictions for the performance of the RHT.

The PHT uses an accumulator matrix just as in the standard Hough Transform. Unlike the PHT, the RHT is designed to exploit the typical sparsity of the accumulator matrix that follows from the small poll size. This is accomplished by using a dynamic data structure, the elements of which roughly correspond to non-empty ("active") accumulator cells. Let A denote the number of active cells in the RHT. With the image and polling models described in this section, we can assume that all pairs that vote for the perfect line contribute to few cells, and that every pair that does not vote for the perfect line creates an active cell (this is true as long as p is not extremely large). Thus, the expected value of the number of active cells is roughly

$$E(A) \approx p\left[1-\left(\frac{\alpha S}{M}\right)^2\right]+1 \approx p, \qquad (12)$$

i.e., close to the number of pairs p.

Table 5 shows the empirical average number of active cells $\overline{A}$, when applying the RHT to the test image shown in Fig. 1, for several poll sizes p (pairs). The ratio $\overline{A}/p$ is also presented (according to the analysis, this ratio should be close to 1). These experiments are in reasonable agreement with the rough prediction provided by Eq. 12.

Table 5
Top row: RHT poll size p (pairs) *Middle row:* Empirical average number of active cells (rounded). *Bottom row:* $\overline{A}/p$. These results were obtained using the test image shown in Fig. 1. As predicted, $\overline{A}/p$ is close to 1, but slowly decreases as p is increased.

p	344	508	775	987	1205
$\overline{A}$	338	495	746	942	1140
$\overline{A}/p$	0.98	0.97	0.96	0.95	0.94

4. Comparison: Computational Cost

Suppose that the image model and the PHT and RHT polling models described in Sections 2 and 3 hold, and that the poll sizes are sufficient to ensure that both algorithms are in reasonable operating points (i.e., achieve small failure probabilities). We proceed to compare the number of PHT samples m and the number of RHT sample pairs p that are required for achieving the *same* probability of failure.

Equal failure probability means that

$$\Pr(s \le 2) = \Pr(l \le 1) \qquad (13)$$

where the left hand side refers to the PHT and the right hand side to the RHT. From equations 5 and 10 we have

$$\left(1-\frac{\alpha S}{M}\right)^{m-2} \cdot \frac{m^2}{2} \cdot \left(\frac{\alpha S}{M}\right)^2 = \left[1-\left(\frac{\alpha S}{M}\right)^2\right]^{p-1} \cdot p \cdot \left(\frac{\alpha S}{M}\right)^2 \qquad (14)$$

Note that for clarity, here (and in the sequel) we make the approximation that for a given image, α, the fraction of real line points that remain "sufficiently close" to the ideal line, is the same in the PHT and the RHT. Taking the logarithm of both sides, using the Taylor approximation $\log(1+x) \approx x$ (for small $|x|$) and assuming that m and p are sufficiently large, we obtain the simple result

$$m \approx \alpha \frac{S}{M} p\,. \qquad (15)$$

Table 6 compares the empirical PHT poll sizes m (points) and the empirical RHT poll sizes p (pairs) that are needed to obtain several failure rates ϵ when operating on the test image shown in Fig. 1. The ratios $\tilde{\alpha} \equiv (m/p)/(S/M)$ are also shown. The analysis predicts that the ratios $\tilde{\alpha}$ should remain constant for various values of ϵ, and that $\tilde{\alpha}$ should be equal to α (which is about 0.7 for both the PHT and the RHT with this image). The empirical findings, in this and other experiments, support the prediction that $\tilde{\alpha}$ is stable, but in our experiments its empirical value is somewhat higher than α.

Table 6
Comparison of the empirical PHT poll sizes m (points) and the empirical RHT poll sizes p (pairs) that are needed to obtain several failure rates ϵ when operating on the test image shown in Fig. 1. The ratios $\tilde{\alpha} \equiv (m/p)/(S/M)$ are also shown.

ϵ	0.3	0.1	0.03	0.01
m	56	68	106	111
p	508	775	987	1205
$\tilde{\alpha} \equiv (m/p)/(S/M)$	1.10	0.88	1.07	0.92

The decision of whether to use the PHT or the RHT in a given application depends, of course, on the computational cost. Suppose that the computational cost of the PHT is proportional to the number of votes[5], and that the overall cost of a single vote is c_{pht}. The total cost of the PHT is then $m \cdot N_\theta \cdot c_{pht}$, where N_θ is the number of accumulators in the θ direction. For the RHT, suppose that the overall cost of a single pair is c_{rht}. Then the total RHT cost is $p \cdot c_{rht}$.

At the points of equal probability of failure $m \approx (\tilde{\alpha}S/M)p$, so at those points we compare

$$\frac{\tilde{\alpha}S}{M} \cdot p \cdot N_\theta \cdot c_{pht} \stackrel{<}{>} p \cdot c_{rht} \qquad (16)$$

Defining

$$T = \frac{c_{rht}}{N_\theta \cdot c_{pht}} ,$$

we obtain that if

$$\tilde{\alpha}\frac{S}{M} > T \qquad (17)$$

i.e., if the "signal to noise" ratio is higher than some threshold, the RHT is cheaper. Otherwise, if

$$\tilde{\alpha}\frac{S}{M} < T \qquad (18)$$

the PHT is more economical.

To illustrate the power of Eqs. 17 and 18, consider the two edge images shown in Fig. 2. They are similar to the image shown in Fig. 1, except for the higher numbers of randomly distributed noise points. Table 7 compares the empirical poll sizes and computing time[6] needed in order to obtain a failure rate of 0.3 when applying the PHT and RHT to the three images. Table 8 is similar to Table 7, but for a failure rate of 0.03. Note that with the RHT we have not been able to achieve a failure rate of 0.03 at all in Fig. 2 (right). The data in both tables shows that the RHT is superior to the PHT in processing Fig. 1 for which $S/M = 0.1$. The performance of the two algorithms is comparable in analyzing Fig. 2 (left), where $S/M = 0.05$. However, the RHT is clearly inadequate for dealing with Fig. 2 (right), with $S/M = 0.025$. The PHT works well on that image.

[5] A finer computational cost model would add fixed initialization costs to the costs of the PHT and the RHT.

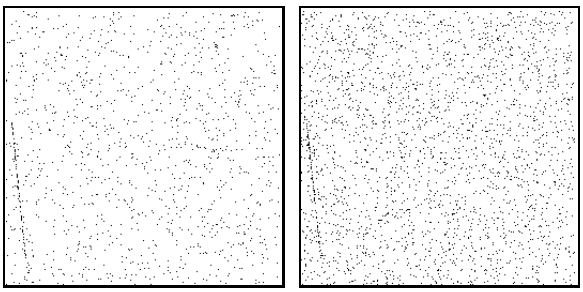

Fig. 2. Noisy versions of the image shown in Fig. 1. *Left:* A 256×256 test image, with $S = 64$ points on a digital line, and $N = 1216$ randomly distributed noise points; $S/M = 0.05$. *Right:* A similar image, but with $N = 2496$ randomly distributed noise points; $S/M = 0.025$.

Table 7
Comparison of the empirical poll sizes and computing time units that are needed to obtain a failure rate of 30% when applying the PHT and the RHT to the three test images shown in Fig. 1 and Fig. 2.

Figure no.	1	2 (left)	2 (right)
S/M	0.1	0.05	0.025
PHT poll m (points)	56	169	758
RHT poll p (pairs)	508	5410	96991
PHT time (units)	0.21	0.41	1.42
RHT time (units)	0.03	0.21	23457.31

[6] Since actual computing time depends on the type of computer used, computing time is presented in the following tables in 'units'. In our experiments one time unit corresponds to one second, on a Sun Ultra 1 Model 200E computer, with 128MB RAM, running Solaris.

Table 8
Comparison of the empirical poll sizes and computing time units that are needed to obtain a failure rate of 3% when applying the PHT and the RHT to the three test images shown in Fig. 1 and Fig. 2. Note that with the RHT we have not been able to achieve a failure rate of 3% at all in Fig. 2 (right).

Figure no.	1	2 (left)	2 (right)
S/M	0.1	0.05	0.025
PHT poll m (points)	106	312	1203
RHT poll p (pairs)	987	9001	∞
PHT time (units)	0.32	0.67	2.16
RHT time (units)	0.05	0.35	∞

5. Comparison: Effect of Location Errors

Suppose that we have the same α for the RHT and the PHT. In order to achieve some small probability of failure ϵ, we need a certain $b = p(\alpha S/M)^2$ in the RHT (Eq. 11) and a certain $c = m(\alpha S/M)$ in the PHT (Eq. 6). To maintain a fixed ϵ as α increases, b and c must stay fixed. Thus, in the RHT

$$p \propto \frac{1}{\alpha^2} \tag{19}$$

while in the PHT

$$m \propto \frac{1}{\alpha} \tag{20}$$

This implies that the RHT is more sensitive than the PHT to location errors.

Our experiments support this conclusion. Consider the two edge images shown in Fig. 3. They are similar to the image shown in Fig. 1, except that errors in the locations of the line points have been introduced. The errors are smaller in Fig. 3 (left) and larger in Fig. 3 (right). Table 9 compares the empirical poll sizes and computing time needed in order to obtain a failure rate of 0.3 when applying the PHT and RHT to the three images. Table 10 is similar to Table 9, but for a failure rate of 0.03. The data in both tables shows that the RHT is superior to the PHT in processing Fig. 1 in which location errors are due only to image quantization. The performance of the two algorithms is comparable in analyzing Fig. 3 (left), with some superiority of the RHT. However, the PHT is greatly superior in dealing with the noisier Fig. 3 (right).

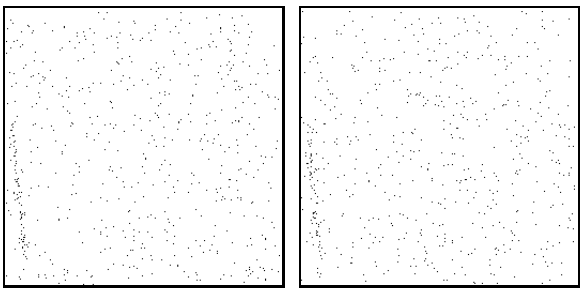

Fig. 3. These images are similar to the image shown in Fig. 1, but with errors in the locations of the line points. The errors in the right image are larger than in the left one.

Table 9
Comparison of the empirical poll sizes and computing time units that are needed to obtain a failure rate of 30% when applying the PHT and the RHT to the three test images shown in Fig. 1 and Fig. 3.

Figure no.	1	3 (left)	3 (right)
Location errors	small	medium	large
PHT poll m (points)	56	85	199
RHT poll p (pairs)	508	2332	15908
PHT time (units)	0.21	0.33	0.42
RHT time (units)	0.03	0.11	0.66

Table 10
Comparison of the empirical poll sizes and computing time units that are needed to obtain a failure rate of 3% when applying the PHT and the RHT to the three test images shown in Fig. 1 and Fig. 3.

Figure no.	1	3 (left)	3 (right)
Location errors	small	medium	large
PHT poll m (points)	106	192	453
RHT poll p (pairs)	987	7833	110651
PHT time (units)	0.32	0.45	0.84
RHT time (units)	0.05	0.30	4.40

6. Conclusions

In this paper a unified theoretical framework for analyzing the performance and limitations of

the Probabilistic Hough Transform (PHT) and the Randomized Hough Transform (RHT) has been established. The conclusions, based on analysis and experiments, can be summarized in clear terms. In the processing of high quality images, both algorithms work well but the RHT is considerably faster than the PHT. However, in the processing of images that are contaminated by noise and errors, the PHT is significantly more robust than the RHT. It still works well and provides valuable computational gains on data for which the RHT is no longer useful.

The results presented in this paper refer to the basic forms of the RHT and the PHT. The performance of various variants of these algorithms, that have been suggested in the literature, may differ. Newer versions of the RHT and the PHT usually perform significantly better than the standard algorithms. We believe, however, that the analytic and experimental framework presented here can be readily generalized to deal with extensions of the generic algorithms, to highlight their advantages and identify their failure mechanisms.

Our analysis concentrated on the detection of a single straight line in a noisy image. Multiple lines can be detected either in parallel or sequentially. In the parallel approach, a single voting session is the basis for the detection of several lines. In the sequential approach, lines are detected one by one: voting takes place, a line is detected, its supporting pixels are removed from the data set and vice versa. The parallel approach may be more efficient when only few lines are to be detected, but the sequential approach seems more suitable for complex images. The RHT was introduced [10] with the sequential approach as an integral part of the algorithm. A sequential PHT was recently considered in [7] (including an experimental comparison with the RHT). Analysis of these strategies using the techniques developed here is possible but is beyond the scope of this paper.

Acknowledgements

The authors thank Mr. Saku Kukkonen for his valuable contributions to implementations and experiments. This study was supported in part by the EC-IS-003 grant and by the Tel Aviv University Internal Research Fund.

References

[1] Duda, R.O. and P.E. Hart (1972). Use of the Hough transform to detect lines and curves in pictures. *Commun. ACM* 15, 11-15.

[2] Kiryati, N., Y. Eldar and A.M. Bruckstein (1991). A probabilistic Hough transform. *Pattern Recognit.* 24, 303-316.

[3] Kälviäinen, H., P. Hirvonen, L. Xu and E. Oja (1995). Probabilistic and non-probabilistic Hough transforms: overview and comparisons. *Image and Vision Computing* 13, 239-252.

[4] Kälviäinen, H. and P. Hirvonen (1997). An extension to the randomized Hough transform exploiting connectivity. *Pattern Recognition Letters* 18, 77-85.

[5] Kälviainen, H., N. Kiryati and S. Alaoutinen (1999). Randomized or probabilistic Hough transform: unified performance evaluation. *Proc. IAPR SCIA*, Kangerlussuaq, Greenland, 259-266.

[6] Leavers, V.F. (1992). The dynamic generalized Hough transform: its relationship to the probabilistic Hough transforms and an application to the concurrent detection of circles and ellipses. *CVGIP: Image Understanding* 56, 381-398.

[7] Matas, J., C. Galambos and J. Kittler (2000). Robust detection of lines using the progressive probabilistic Hough transform. *Computer Vision Image Understanding* 78, 119-137.

[8] Soffer, M. and N. Kiryati (1998). Guaranteed convergence of the Hough transform. *Computer Vision Image Understanding* 69, 119-134.

[9] Shaked, D., O. Yaron and N. Kiryati (1996). Deriving stopping rules for the probabilistic Hough transform by sequential analysis. *Computer Vision Image Understanding* 63, 512-526.

[10] Xu, L., E. Oja and P. Kultanen (1990). A new curve detection method: randomized Hough transform (RHT). *Pattern Recognition Letters* 11, 331-338.

[11] Xu, L. and E. Oja (1993). Randomized Hough transform: basic mechanisms, algorithms and computational complexities. *CVGIP: Image Understanding* 57, 131-154.

[12] Ylä-Jääski, A. and N. Kiryati (1994). Adaptive termination of voting in the probabilistic circular Hough transform. *IEEE Trans. Pattern Anal. Mach. Intell.* 16, 911-915.